

DRAFT

High Resolution Identification of Protein-DNA Binding Events and Quality Control for ChIP-exo data

Dongjun Chung⁶, Rene Welch¹, Irene Ong³, Jeffrey Grass^{3,4}, Robert Landick^{3,4,5} and Sündüz Keleş^{1,2*}

*Correspondence:
keles@stat.wisc.edu

¹Department of Statistics,
University of Wisconsin Madison,
1300 University Avenue, Madison,
WI

Full list of author information is
available at the end of the article

Abstract

Recently, ChIP-exo has been developed to investigate protein-DNA interaction in higher resolution compared to popularly used ChIP-Seq. Although ChIP-exo has drawn much attention and is considered as powerful assay, currently, no systematic studies have yet been conducted to determine optimal strategies for experimental design and analysis of ChIP-exo. In order to address these questions, we evaluated diverse aspects of ChIP-exo and found the following characteristics of ChIP-exo data. First, the background of ChIP-exo data is quite different from that of ChIP-Seq data. However, sequence biases inherently present in ChIP-Seq data still exist in ChIP-exo data. Second, in ChIP-exo data, reads are located around binding sites much more tightly and hence, it has potential for high resolution identification of protein-DNA interaction sites, and also the space to allocate the reads is greatly reduced. Third, although often assumed in the ChIP-exo data analysis methods, the “peak pair” assumption does not hold well in real ChIP-exo data. Fourth, spatial resolution of ChIP-exo is comparable to that of PET ChIP-Seq and both of them are significantly better than resolution of SET ChIP-Seq. Finally, for given fixed sequencing depth, ChIP-exo provides higher sensitivity, specificity and spatial resolution than PET ChIP-Seq.

In this article we provide a quality control pipeline which visually assess ChIP-exo biases and calculates a signal-to-noise measure. Also, we updated dPeak [1], which makes a striking balance in sensitivity, specificity and spatial resolution for ChIP-exo data analysis.

Keywords: ChIP-exo; QC; TFBS; BS identification on High-Res

List of Figures

- 1 Strand cross-correlation curves for σ^{70} samples. The “phantom peak” and the summit that corresponds to the read and fragment length respectively are confounded, due to the exonuclease enzyme digestion. 7
- 2 Diagram of the ChIP-exo Quality control pipeline [this is a placeholder]. The genome is partitioned into several regions by removing the empty segments and for each regions we calculate a collection of QC indicators. 7
- 3 Using the mouse-FoxA1 experiment from [3]: A) Hexbin plots of ARC against URCR, in general we can see a slight separation into two strong arms, one corresponds to low ARC and varying URCR, and for the other URCR decreases as ARC increases B) Boxplots of the local-NSC stratified by nr. of reads mapped to only one position in the regions for the ChIP-exo experiments divided by condition and biological replicate and C) Boxplots of the a set of ERR336942 regions, stratified as in (B) with the local-NSC calculated with the different biological replicates. 9
- 4 Strand imbalance QC plots for the same data as in figure 3. A) FSR distribution quantiles as the lower depth regions are being filtered out, all quantiles approach to the median as the lower bound increases. B) Stacked histogram with the proportion of regions that are formed by two strands or only one, in a good sample the single-stranded regions are going to be filtered out quickly as in the middle row. 10
- 5 A) ChIP signal in ChIP-exo was linearly related to that in PET ChIP-Seq data in the region with high ChIP tag counts. In contrast, there were clear differences in their background distribution, where several ChIP-exo background regions were empty. B) In ChIP-exo data, strands of reads were significantly less balanced in the regions with potential binding sites compared to SET ChIP-Seq data. C) ChIP tag counts increase linearly as mappability scores increases. D) ChIP tag counts increase linearly as GC content score increases when GC content is less than 0.6 and then ChIP tag counts decrease as GC content increases. 11
- 6 Comparison of (A) sensitivity and (B) resolution between ChIP-exo and ChIP-Seq data. Sensitivity is defined as the proportion of RegulonDB annotations identified using each data. Resolution is defined as the distance between RegulonDB annotation and its closest prediction. C) δ parameter in dPeak measures average distance of the reads to their respective binding site. In ChIP-exo data, reads were located much closer to the binding site than in SET ChIP-Seq. D) σ parameter measure the dispersion of reads around each binding site. In ChIP-exo data, reads showed less variation around the their respective binding sites compared to SET ChIP-Seq. 13

7 Comparison of the number of candidate regions (A), predicted events
 (B), identified targets (C) and resolution (D) among ChIP-exo, PET
 ChIP-Seq and SET ChIP-Seq. RegulonDB annotations are consid-
 ered as a gold standard. A gold standard was considered identified if
 a BS was estimated inside a 15 bp window around it 14

8 Hexbin plots of ARC vs URCR for each region after partitioning the
 genome. In A and B the regions with reads mapped to at most 10
 and 30 positions respectively where not considered. ARC is defined
 as the ratio of the nr. of reads and the width of a region and URCR is
 the ratio of the number of unique position where the reads are being
 allocated and the number of reads in a region. 17

1 Background

ChIP-exo (Chromatin Immunoprecipitation followed by exonuclease digestion and next generation sequencing) Rhee and Pugh ([2]) is the state-of-the-art experiment developed to attain single base-pair resolution of protein binding site identification and it is considered as a powerful alternative to popularly used ChIP-Seq (Chromatin Immunoprecipitation coupled with next generation sequencing) assay. ChIP-exo experiments first capture millions of DNA fragments (150 - 250 bp in length) that the protein under study interacts with using random fragmentation of DNA and a protein-specific antibody. Then, exonuclease is introduced to trim 5' end of each DNA fragment to a fixed distance from the bound protein. As a result, boundaries around the protein of interest constructed with 5' ends of fragments are located much closer to bound protein compared to ChIP-Seq. This step is unique to ChIP-exo and could potentially provide significantly higher spatial resolution compared to ChIP-Seq. Finally, high throughput sequencing of a small region (25 to 100 bp) at 5' end of each fragment generates millions of reads or tags.

While the number of produced ChIP-exo data keeps increasing, characteristics of ChIP-exo data and optimal strategies for experimental design and analysis of ChIP-exo data are not fully investigated yet, including issues of sequence biases inherent to ChIP-exo data, choice of optimal statistical methods, and determination of optimal sequencing depth. However, currently the number of available ChIP-exo data is still limited and their sequencing depths are still insufficient for such investigation. To address this limitation we gathered ChIP-exo data from diverse organisms: CTCF factor in human [2]; ER factor in human and FoxA1 factor in mouse [3]; and generated σ^{70} factor in *Escherichia coli* (E. Coli) under aerobic (+O₂) condition, and treated by rifampicin by 0 and 20 minutes.

DNA libraries generated by the ChIP-exo protocol seem to be less complex than the libraries generated by ChIP-Seq [4]. Hence, most of current QC guidelines [5] may not be applicable on ChIP-exo, additionally to our knowledge there are not established quality control pipelines for ChIP-exo. To address this challenge, we suggest a collection of quality control visualizations to understand which biases are present in ChIP-exo data. Previous ChIP-exo analysis used ChIP-Seq samples to compare the resolution between experiments ([2], [6], [3]); in [7], Carroll et. al. studied the use of the Strand-Cross Correlation (SCC) [8] and showed that by filtering blacklisted regions the estimation of the SCC is improved. However, this method requires to know blacklisted regions in advance which may not be available, additionally using SCC may not be useful since the peaks that are attained at the read and fragment length are confused in a typical ChIP-exo SCC curve. In our pipeline we propose two out-the-shelf analysis: An enrichment plot and the local normalized SCC coefficient.

In order to archive the potential benefits of ChIP-exo on protein binding site identification, it is critical to understand which are the important characteristics of ChIP-exo data and to use algorithms that could fully utilize information available in ChIP-exo data. Rhee and Pugh [2] discussed that reads in the forward and reverse strand might construct peak pairs around bound protein, of which heights were implicitly assumed to be symmetric. Hence, they used the “peak pair method” that predicts the midpoint of two modes of peak pairs as potential binding site.

Mace [9], CexoR [10] and peakzilla [11], recently developed ChIP-exo data analysis methods, are also based on this peak pair assumption. However, appropriateness of such assumption was not fully evaluated in the literature yet. Furthermore, it is still unknown which factors could affect protein binding site identification using ChIP-exo data. In order to address this problem, we investigated various aspects of ChIP-exo data by contrasting them with their respective ChIP-Seq experiments.

Currently, research on statistical methods for ChIP-exo data is still in its very early stage. Although many methods have been proposed to identify protein binding sites from ChIP-Seq data (reviewed in [12] and [13]), such as MACS [14], CisGenome [15] and MOSAiCS [16], these approaches reveal protein binding sites in lower resolution, i.e., at an interval of hundreds to thousands of base pairs. Furthermore, they report only one “mode” or “predicted binding location” per peak. Hence, these methods are not appropriate to evaluate the potential of ChIP-exo data for high resolution identification of protein binding sites. More recently, deconvolution algorithms such as Deconvolution [17], GEM [18] (an improved version of [19]) and PICS [20] have been proposed to identify binding sites in higher resolution using ChIP-Seq data. However, most of them are still not tailored for ChIP-exo and PET and SET ChIP-Seq data in a unified framework and as a result, currently available methods are not appropriate for fair comparison between ChIP-exo and ChIP-Seq. To address these limitations, we developed an improved dPeak [1], a high resolution binding site identification (deconvolution) algorithm that we previously developed for PET and SET ChIP-Seq data, so that it can also handle ChIP-exo data. The dPeak algorithm implements a probabilistic model that accurately describes the ChIP-exo and ChIP-Seq data generation process.

In this paper, we demonstrate that the “peak pair” assumption of Rhee and Pugh [2] does not hold well in real ChIP-exo data. Furthermore, we found that when we analyze ChIP-exo data from eukaryotic genomes, it is important to consider sequence biases inherent to ChIP-exo data, such as mappability and GC content in order to improve sensitivity and specificity of binding site identification. We evaluated several methods to identify binding events and dPeak outperforms or performs competitively respect to GEM and MACE when analyzing ChIP-exo data. More importantly, when comparable number of reads is used for both ChIP-exo and ChIP-Seq, dPeak coupled with ChIP-exo data provides resolution comparable to PET ChIP-Seq and both significantly improve the resolution of protein binding site identification compared to SET-based analysis with any of the available methods.

2 Results and discussion

2.1 Deeply sequenced E.Coli σ^{70} ChIP-exo and ChIP-Seq data

σ^{70} factor is a transcription initiation factor of housekeeping genes in E. coli. In E. coli genomes, many promoters contain multiple transcription start sites (TSS) and these TSS are often closely spaced (10–150 bp). These closely spaced binding sites are considered to be multiple “switches” that differentially regulate gene expression under diverse growth conditions [21], [22]. Therefore, investigation of ChIP-exo’s potential for identification and differentiation of closely spaced binding sites are invaluable for elucidating the transcriptional networks of prokaryotic genomes.

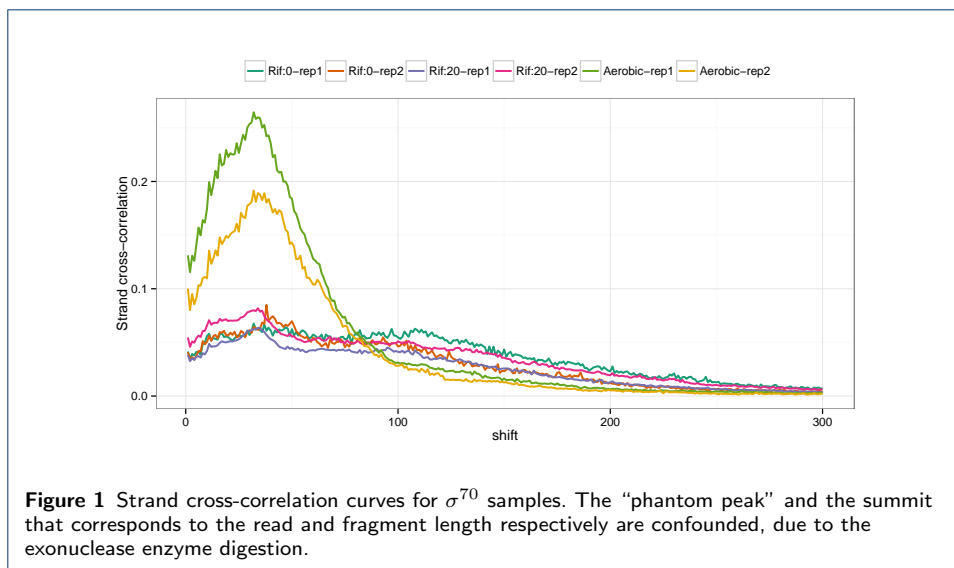
2.2 Current guidelines and quality metrics

We calculated the most commonly used quality indicators for ChIP-Seq data, which are listed in table 1. The PBC and NSC were calculated as defined in [5] and the SSD was calculated as defined in [23]. Additionally, we calculated the FSR to compare the number of fragments in each strand. A few conclusions that we may get by observing the PBC in table 1 are all the samples have a quite low library complexity, hence it would be suggested to repeat the experiment.

IP	Organism	Condition	Rep.	Nr. reads	PBC	SSD	NSC
σ^{70}	E.Coli	Rif-0min	1	960,256	0.2823	0.0361	10.29
σ^{70}	E.Coli	Rif-0min	2	2,247,295	0.2656	0.1091	25.08
σ^{70}	E.Coli	Rif-20min	1	1,940,387	0.2698	0.0820	17.69
σ^{70}	E.Coli	Rif-20min	2	4,229,574	0.2153	0.1647	14.11
FoxA1	Mouse	NA	1	22,210,461	0.6562	9.12×10^{-5}	21.452
FoxA1	Mouse	NA	2	22,307,557	0.7996	7.94×10^{-5}	60.661
FoxA1	Mouse	NA	3	22,421,729	0.1068	1.31×10^{-4}	72.312
ER	Human	NA	1	9,289,835	0.8082	3.64×10^{-5}	19.843
ER	Human	NA	2	11,041,833	0.8024	4.6×10^{-5}	21.422
ER	Human	NA	3	12,464,836	0.8203	4.89×10^{-5}	19.699
CTCF	Human	NA	1	48,478,450	0.4579	1.29×10^{-4}	15.977

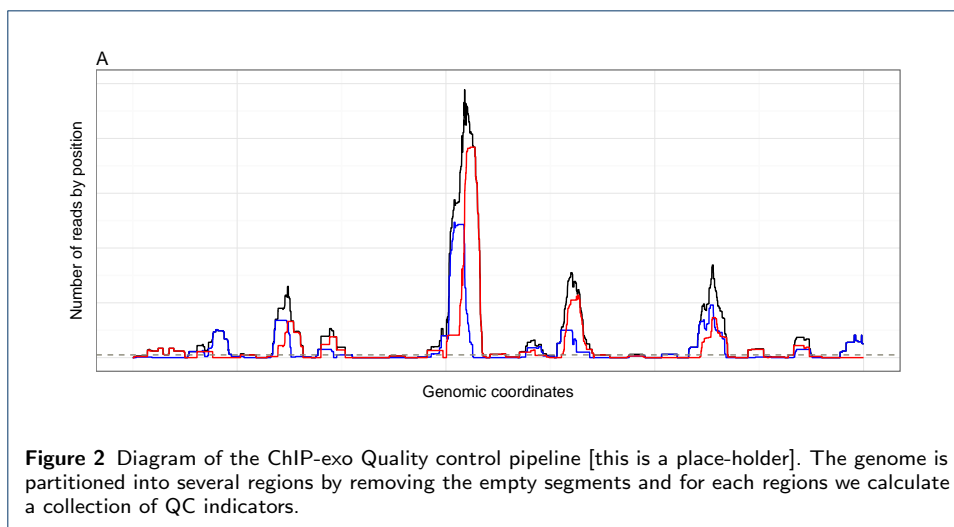
Table 1 Usual quality control indicators applied to our σ^{70} samples. PBC stands PCR-bottleneck coefficient, SSD for standardized standard deviation, FSR for forward strand ratio, NSC for normalized strand cross-correlation coefficient. We omitted the RSC (relative strand cross-correlation since ChIP-exo experiments don’t usually have an accompanying input file) [note: I need to change the table, due the alignment issue]

It is of special importance to notice that the values of PBC are quite low, hence these experiments would be repeated if they were considered as ChIP-Seq experiments. On the other hand, in a good ChIP-Seq experiment the strand cross-correlation is maximized at the fragment length and there is also a “phantom peak” at the sample’s read length ([5] and [8]). However, in ChIP-exo’s case these two peaks are confounded. Hence an enrichment measure based in the strand cross-correlation such as NSC or RSC is harder to interpret. In figure 1 we plotted the SCC curves for σ^{70} ChIP-exo experiments used to calculate the NSC and RSC values in table 1. According to ENCODE’s quality metrics, NSC values close to one corresponds to low enrichment samples or bad quality datasets, hence in our case the last four samples would be considered to have higher quality than they actually have. On the other hand, all PBC values are considerably low and correspond to samples with severe bottlenecking issues, in particular we are going to show that for the first two samples we are obtaining a smaller resolution and identifying a comparable number of targets as in ChIP-Seq PET experiments.



2.3 ChIP-exo Quality Control pipeline

Figure 2 shows a flowchart for the ChIPexoQC pipeline. Which basically partitions the genome by keeping the non-digested ChIP-exo regions. Then, for each region it calculates a series of statistics. Finally, it creates several visualizations designed to assess the quality levels of a ChIP-exo sample.



2.3.1 Enrichment and library complexity in ChIP-exo data

In ChIP-exo experiments, the background is often digested by the exonuclease enzyme, therefore to determine the sample’s quality is necessary to address the balance between the enrichment and library complexity. To diagnose this, we considered the Average Read Coverage (ARC) and the Unique Read Coverage Rate (URCR) which are defined as:

$$\text{ARC} = \frac{\text{Nr. of reads in the region}}{\text{Width of the region}}$$

$$\text{URCR} = \frac{\text{Nr. of reads mapped to only one position in the region}}{\text{Nr. of reads in the region}}$$

Using the mouse-FoxA1 experiment from [3] and the relationship between this two quantities, library complexity and sample enrichment was explored. Figure 3A shows hexbin plots illustrating the interaction between these two quantities. Notice how there are two strong arms in each panel: The first one corresponds to regions with low ARC values and varying URCR values across the $(0,1]$ interval, while the second one shows a decreasing trend in URCR as ARC increases. When an experiment shows a higher degree of enrichment, then the separation of this two arms is more noticeable, since the second arm corresponds to possibly enriched regions (8A and 8B).

Figure 3B shows box plots of the local-NSC on regions of the three replicates, stratified by the number of reads mapped exactly to one position for all σ^{70} ChIP-exo experiments; The high stratum is defined by regions consisting of more than 100 unique positions, the medium stratum for regions where the number of unique position is on the $(50,100)$ range and the low stratum in the $(20,50)$ range. For each stratum and biological replicate, we sampled 400 regions whenever possible (in the opposite case, all the regions in the category were considered) and calculated the local-NSC for those regions. For all three replicates, it is shown an increasing trend as the number of unique position increases, which means that the local-NSC is an effective indicator of library complexity. Figure 3C shows the local-NSC coefficient calculated for the same set of regions, stratified by the number of unique positions in the regions of ERR336942 using the same criteria as before. In the high panel it is shown that the ERR336942 sample performs slightly better than ERR336956 and both outperform ERR336935, this agrees with 3A, where only in the left-most panel doesn't seem to be a separation between the low ARC arm and the other.

2.3.2 Strand imbalance in ChIP-exo data

The strand imbalance assessment is based in the observation that the enriched regions usually have a higher concentration of fragments, therefore we examined the FSR (defined as the ratio of the number of forward stranded reads divided by the total number of reads in a given region) as the region with lower depth are being filtered out. This indicator is of particular importance, since several methods rely on the “peak-pair” assumption. In table 1, we calculated the FSR and noticed that for all the samples, it's value is close to 0.5, which means that there are roughly the same amount of reads in both strands. However, figure 5B shows that this value is not representative of the sample locally, therefore the assumption doesn't hold in practice.

In order to assess the strand imbalance we created the following visualization presented in figure 4. A) shows the FSR's behavior as lower depth regions are being filtered out, while B) shows which percentage of the regions are composed by fragments of both strands or only one (forward or backward). As the number of

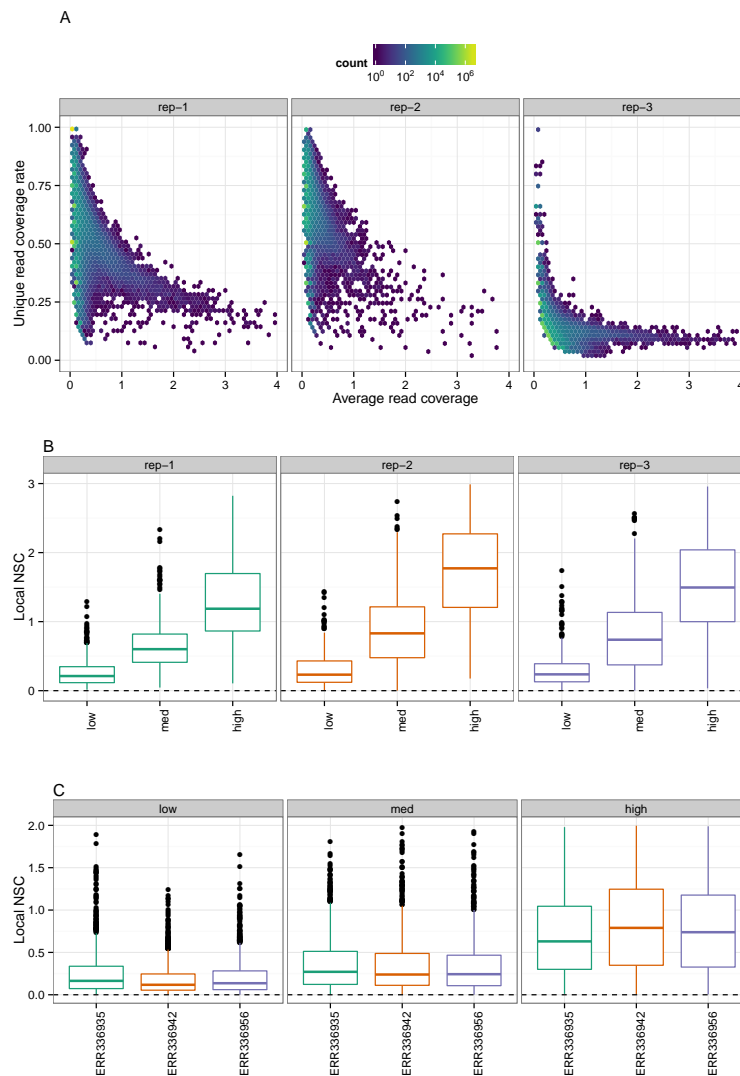
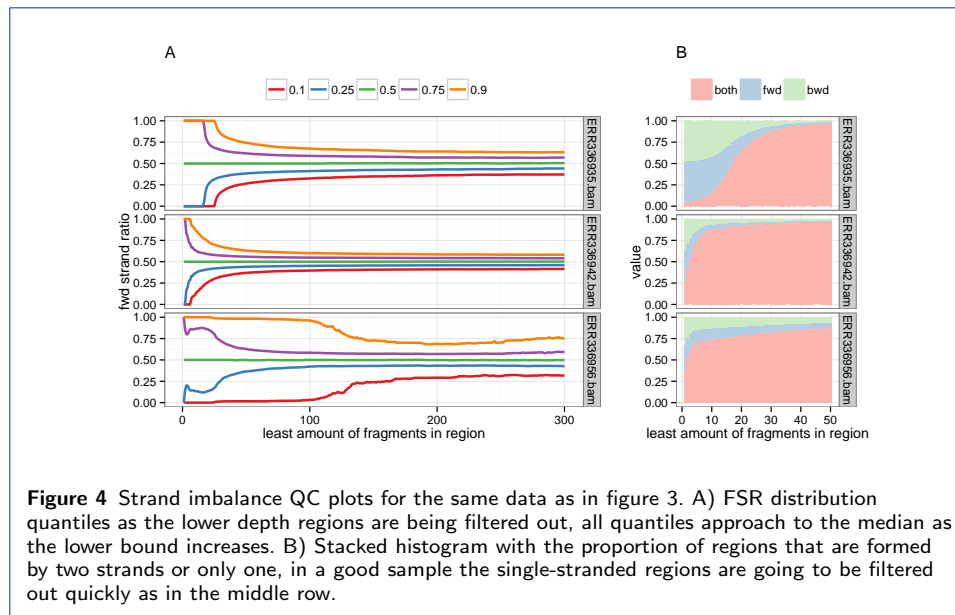


Figure 3 Using the mouse-FoxA1 experiment from [3]: A) Hexbin plots of ARC against URCR, in general we can see a slight separation into two strong arms, one corresponds to low ARC and varying URCR, and for the other URCR decreases as ARC increases B) Boxplots of the local-NSC stratified by nr. of reads mapped to only one position in the regions for the ChIP-exo experiments divided by condition and biological replicate and C) Boxplots of the a set of ERR336942 regions, stratified as in (B) with the local-NSC calculated with the different biological replicates.

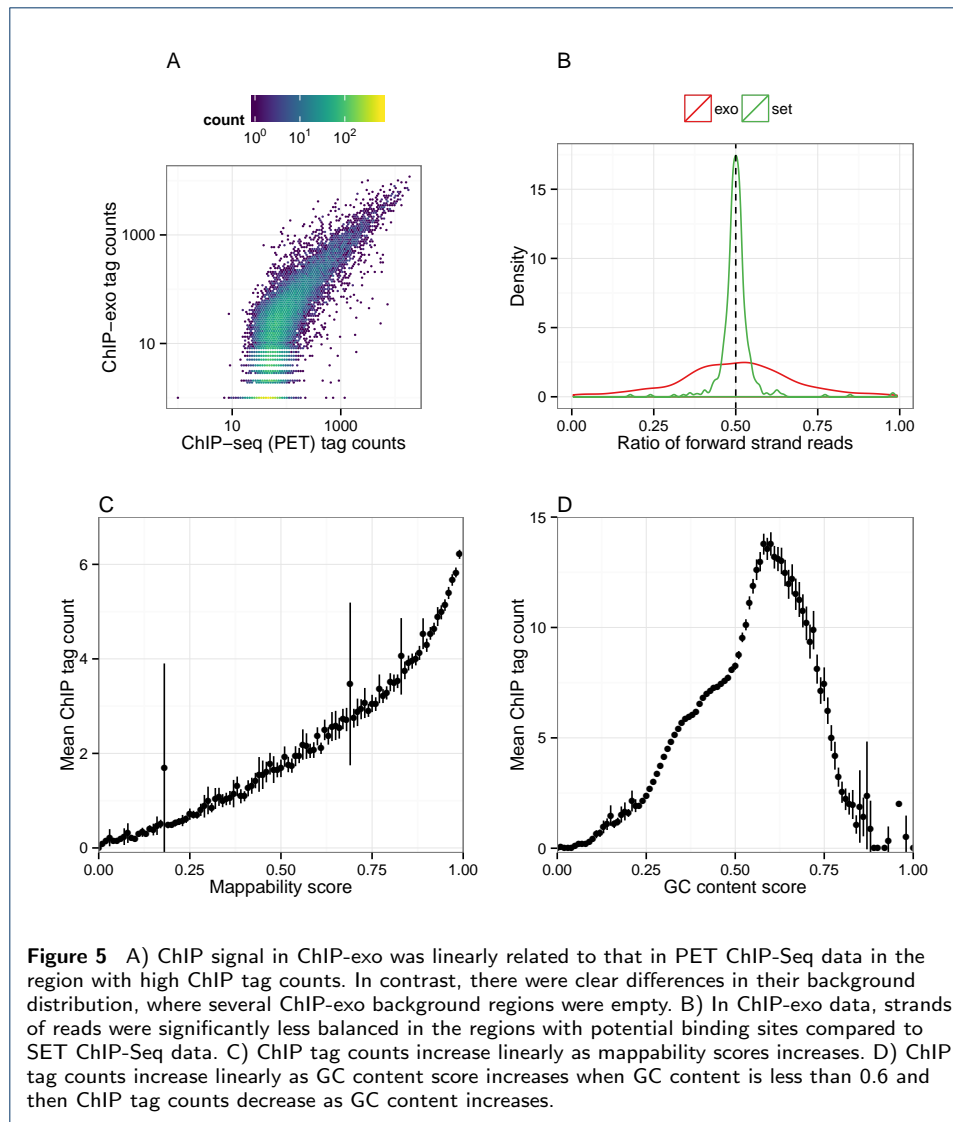
reads per region's lower bound increases, the quantiles tend to approach the median. To evaluate this statement, for each replicate of the FoxA1 dataset, we divided the regions formed by at least 100 fragments into the ones that overlap with any of the sample's peaks. The p.value for ERR336935 is 0.1039, for ERR336942 is 0.0064 and for ERR336956 is 0.0871. This shows that only the middle sample from figure 4 is the least imbalance sample from the three, while the other two still show a higher imbalance at the 100 level.



2.4 Comparison with ChIP-Seq data

We first compared various factors that could affect binding site identification between ChIP-exo and ChIP-Seq data. In order to compare distribution of signal and background between ChIP-exo and ChIP-Seq data, we calculated ChIP tag counts across the genome by counting the number of reads mapping to each of 150 non-overlapping window after extending reads by 150 to their 3' end directions. ChIP tag counts in ChIP-exo data were linearly related to ChIP tag counts in ChIP-Seq data for the regions with high ChIP tag counts (Figure 5A). This implies that signals for potential binding sites are well reproducible between ChIP-exo and ChIP-Seq data. On the other hand, there was clear difference in the background distribution between them. In ChIP-Seq data reads were almost uniformly distributed over background (non-binding) regions and the ChIP tag counts in there regions were significantly larger than zero. In contrast, in ChIP-exo data, there was larger variation in ChIP tag counts among background regions and ChIP tag counts were much lower in these regions compared to ChIP-Seq data. There were also large proportion of regions without any read in ChIP-exo data. These results indicate that background distribution of ChIP-exo data is less homogeneous than that of ChIP-Seq data.

We next evaluated the “peak pair” assumption from Rhee and Pugh [2], MACE [9], CexoR, [10] and peakzilla [11], i.e. a peak of reads in the forward strand is usually paired with a peak of reads in the reverse strand that is located in the other site of the binding site. In order to evaluate this assumption, we reviewed the proportion of reads in the forward strand in candidate regions (i.e. regions with at least one binding site) in σ^{70} ChIP-exo data. We found that strands of reads were much less balanced in ChIP-exo data than in ChIP-Seq data in these regions with potential binding sites (Fig. 5B) and this indicates that the peak pair assumption might not hold in real ChIP-exo data.



2.4.1 ChIP-exo data from eukaryotic genome shows clear sequence biases

We evaluated ChIP-exo data for CTCF factor from human genome [2] to investigate issues specific to eukaryotic genomes for binding sites identification. Figures 5C and 5D display the bin-level average read counts against mappability and GC content. Each data point is obtained by averaging the read counts across bins with the same mappability or GC content. These results indicate that binding site identification in ChIP-exo sample might also benefit from the use of methods that take into account of apparent sequence biases such as mappability and GC content.

2.4.2 Comparison with ChIP-Seq data using dPeak

Figure 6 shows different comparisons among ChIP-exo, PET ChIP-Seq and SET ChIP-Seq. A RegulonDB annotation was considered identified if the distance between it and dPeak binding site estimate was at most of 20 bp. That way, the sensitivity is defined as the proportion of RegulonDB annotations identified in a peak. In figure 6A can be seen that the sensitivity of all protocols increases as the

average distance between binding sites does. Despite that when the binding events in a peak are closer to each other, both ChIP-exo and PET ChIP-Seq are comparable, as the distance increases ChIP-exo identifies a higher proportion of the RegulonDB annotations; additionally SET ChIP-Seq is significantly less sensible than both ChIP-exo and PET ChIP-Seq. In figure 6B the distance between a RegulonDB annotation to its closest prediction is compared for ChIP-exo, PET and SET ChIP-Seq; while the first two are comparable, both outperform SET ChIP-Seq.

In figures 6C and 6D, we observe the behavior of dPeak’s estimated parameters for single end data (both ChIP-exo and ChIP-Seq). The δ parameter measures the distance from the 5’ end of the fragment to its respective binding event and the σ parameter indicates the fragments distribution variability around their respective binding sites (more information in [1]). For both parameters, it can be seen that the ChIP-exo estimates are smaller than the SET ChIP-Seq estimates in average, which agrees with the fact that the sample reads are allocated more tightly around the binding events in ChIP-exo data. Hence we can conclude that the peaks shape is quite different between ChIP-exo and SET ChIP-Seq.

2.5 Recommendations for the design of ChIP-exo experiments

We sampled a fixed amount of fragments for each of the ChIP-exo, PET ChIP-Seq and SET ChIP-Seq datasets of the σ^{70} sample in aerobic conditions. For each sampled dataset we applied our lower-to-higher resolution pipeline by calling peaks with MOSAiCS [16] and then deconvolving the binding events by using dPeak [1]. For the ChIP-exo datasets we called peaks by using GC-content and mappability with MOSAiCS, and for the ChIP-Seq datasets we used their respective Input samples.

Figure 7 shows the behavior of each data type when their depth is fixed. It is remarkable that even when the number of candidate peaks or the number of predicted events is lower for ChIP-exo, it outperforms both PET and SET ChIP-Seq in the number of identified targets and resolution. This may suggest that with ChIP-exo less false positive peaks are being called and that when the targets are being identified, dPeak estimates binding locations closer to the true location. Additionally, we can see that as the read depth increases all four indicators do so as well, which may indicate that with ChIP-exo a smaller amount of reads is necessary to identify a higher number of targets, but it may also be possible that this is an artifact occurring due to ChIP-exo’s lower library complexity.

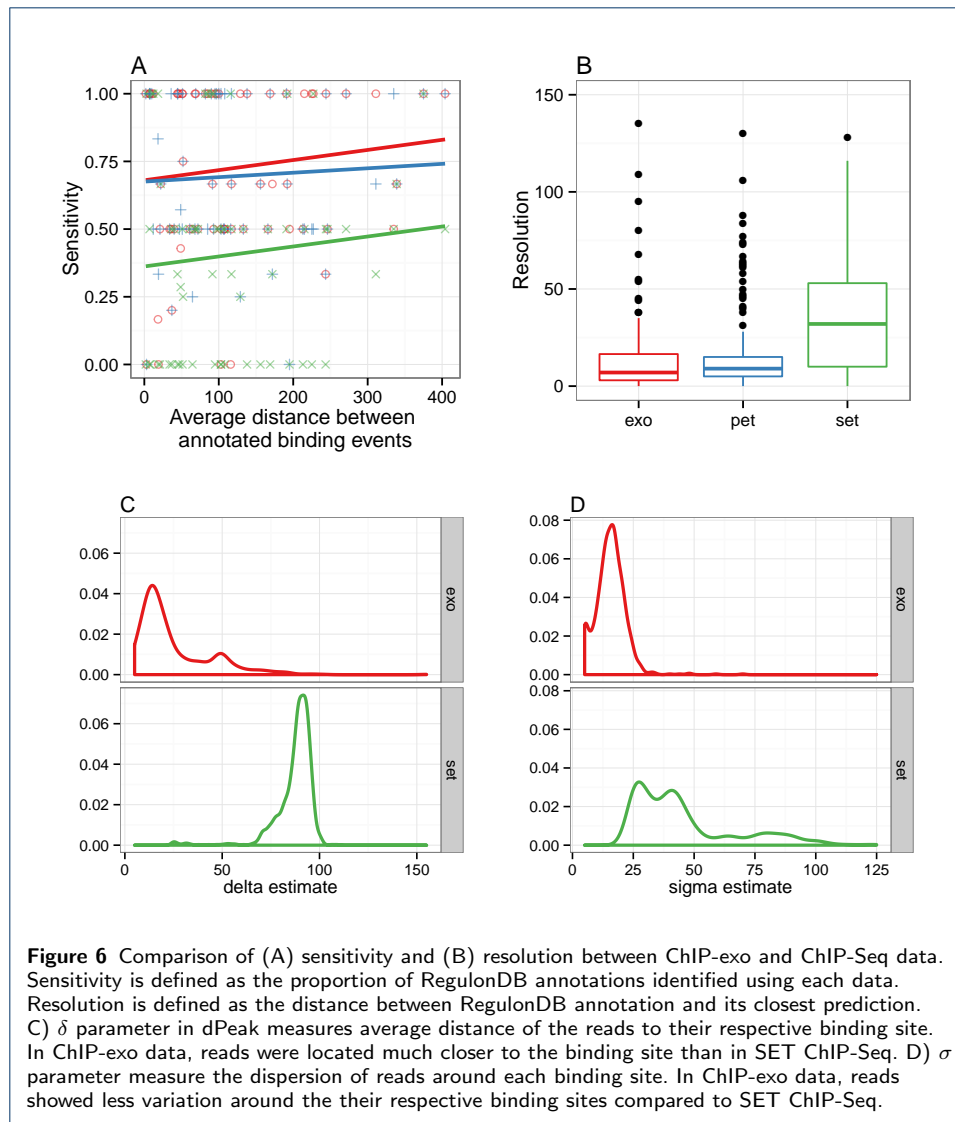
2.6 dPeak outperforms competing methods in discovering closely space binding event from ChIP-exo and ChIP-Seq data

I plan to update this analysis, since the dpeak’s new strategy seems to decrease resolution. Also, Apex was updated into MACE, so I think it could be better to add that method instead.

Also need to make an equivalente to Fig5 in manuscript

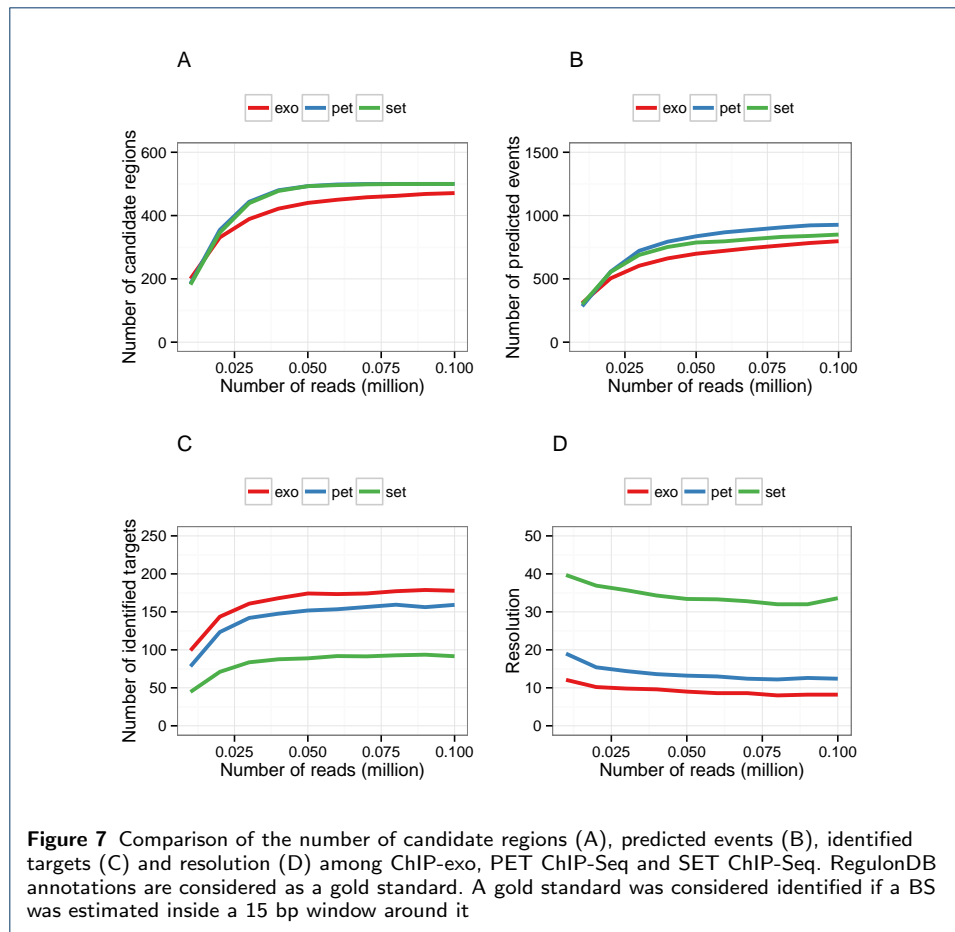
3 Conclusions

We provide a ChIP-exo QC pipeline capable of assess the balance between enriched samples and low complexity regions. It is shown that the “peak-pair” assumption



doesn't hold in practice and we provide two out-of-the-box visualization capable to assess the strand imbalance in a ChIP-exo experiment.

We updated the dPeak algorithm from [1] and showed that ChIP-exo is comparable in resolution and sensitivity with PET ChIP-Seq and outperforms SET ChIP-Seq. ChIP-exo compared with PET and SET ChIP-Seq at fixed depth sample is able to identify more targets at a lower resolution. We compared dPeak with another algorithms to estimate binding locations in ChIPexo data, dPeak is comparable to MACE and outperforms GEM in resolution. dPeak provided a striking balance in sensitivity, specificity and spatial resolution for ChIP-exo analysis.



4 Methods

4.1 Growth conditions

4.2 ChIP-exo experiments

4.3 Library preparation, sequencing and mapping of sequencing reads

4.4 Method comparison with ChIP-exo

We considered dPeak Chung et al. [1], GEM Guo et al. [18] and MACE Wang et al. [9] for ChIP-exo data analysis. For the dPeak algorithm, we used the R package *dPeak* version 1.0.0, which is available from <http://dongjunchung.github.io/dpeak/>. For the GEM algorithm we used its Java implementation version 0.9, which is available from <http://cgs.csail.mit.edu/gem/>. For the MACE algorithm, we used its Python implementation version 1.0, which is available from <http://dldcc-web.brc.bcm.edu/lilab/MACE/docs/html/>. For the PEAKZILLA algorithm, we used its Python implementation, which is available in <http://www.starklab.org/data/peakzilla/>. Candidate regions for dPeak were identified for each replicate of ChIP-exo data using the MOSAiCS algorithm Kuan et al. [16] (one sample analysis using false discovery rate of 0.0001) implemented as an R package *mosaics* 2.4 (available from *Bioconductor* <https://www.bioconductor.org/packages/release/bioc/html/mosaics.html>). We further filtered out candidate region with average ChIP tag count less than 3,000 to avoid potential false positives based in exploratory analysis. These regions were also explicitly provided to the

GEM algorithm as candidate regions. Default tuning parameters were used during model fitting for all methods. We tried to use the CexoR algorithm with its R implementation version 1.8.0 available from <http://bioconductor.org/packages/release/bioc/html/CexoR.html>, but it returned an error every time we used it.

4.5 Local-NSC

The local strand cross-correlation is defined as:

$$\text{local-NSC} = \frac{\max_{x_\delta} f(x_\delta)}{\sigma}$$

$$y_\delta = f(x_\delta) + \sigma \epsilon_\delta$$

where f is calculated by fitting a local polynomial regression model over the strand cross-correlation calculated using exclusively the fragments that overlap a pre-defined genomic region, y_δ is the correlation of the forward and backward coverages when one is shifted x_δ bp towards their 3' end.

The local polynomial model was fitted using the *loess* function from the R software version 3.2.1 using the default tuning parameters.

Author details

¹Department of Statistics, University of Wisconsin Madison, 1300 University Avenue, Madison, WI. ²Department of Biostatistics and Medical Informatics, University of Wisconsin Madison, 600 Highland Avenue, Madison, WI. ³Great Lakes Bioenergy Research Center, University of Wisconsin Madison, 1552 University Avenue, Madison, WI. ⁴Department of Biochemistry, University of Wisconsin Madison, 433 Babcock Drive, Madison, WI. ⁵Department of Bacteriology, University of Wisconsin Madison, 1550 Linden Drive, Madison, WI. ⁶Department of Public Health Sciences, Medical University of South Carolina, 135 Cannon Street, Charleston, SC.

References

- Chung, D., Park, D., Myers, K., Grass, J., Kiley, P., Landick, R., Keleş, S.: dpeak, high resolution identification of transcription factor binding sites from pet and set chip-seq data. *PIOS, Computational Biology* (2013)
- Rhee, H.S., Pugh, F.: Comprehensive genome-wide protein-dna interactions detected at single-nucleotide resolution. *Cell* (2011)
- Serandour, A., Gordon, B., Cohen, J., Carroll, J.: Development of and illumina-based chip-exonuclease method provides insight into foxa1-dna binding properties. *Genome Biology* (2013)
- Mahony, S., Franklin, P.B.: Protein-dna binding in high-resolution. *Critical Reviews in Biochemistry and Molecular Biology* (2015)
- Landt, S., Marinov, G., Kundaje, A., Kheradpour, P., Pauli, F., Batzoglou, S., Bernstein, B., Bickel, P., Brown, J., Cayting, P., Chen, Y., DeSalvo, G., Epstein, C., Fisher-Aylor, C., Euskirchen, G., Gerstein, M., Gertz, J., Hartemink, A., Hoffman, M., Iyer, V., Jung, Y., Karmakar, S., Kellis, M., Kharchenko, P., Li, Q., Liu, T., Liu, S., Ma, L., Milosavljevic, A., Myers, R., Park, P., Pazin, M., Perry, M., Raha, D., Reddy, T., Rozowsky, J., Shores, N., Sidow, A., Slatery, M., Stamatoyannopoulos, J., Tolstorukov, M., White, K., Xi, S., Farnham, P., Lieb, J., Wold, B., Snyder, M.: Chip-seq guidelines and practices of the encode and modencode consortia. *Genome Research* (2012)
- Rhee, H.S., Pugh, F.: Chip-exo a method to identify genomic location of dna-binding proteins at near single nucleotide accuracy. *Current Protocols in Molecular Biology* (2012)
- Carroll, T., Liang, Z., Salama, R., Stark, R., de Santiago, I.: Impact of artifact removal on chip quality metrics in chip-seq and chip-exo data. *Frontiers in Genetics, Bioinformatics and Computational Biology* (2014)
- Kharchenko, P., Tolstorukov, M., Park, P.: Design and Analysis of ChIP-seq Experiments for DNA-binding Proteins
- Wang, L., Chen, J., Wang, C., Uusküla-Reimand, L., Chen, K., Medina-Rivera, A., Young, E.J., Zimmermann, M.T., Yan, H., Sun, Z., Zhang, Y., Wu, S.T., Huang, H., Wilson, M.D., Kocher, J.-P.A., Li, W.: Mace: model based analysis of chip-exo. *Nucleic Acids Research* (2014)
- Madrigal, P. *EMBnet.journal* (2015)
- Bardet, A.F., Steinmann, J., Bafna, S., Knoblich, J.A., Zeitlinger, J., Stark, A.: Identification of transcription factor binding sites from chip-seq data at high resolution. *Bioinformatics* (2013)
- Wilbanks, E., Facciotti, M.: Evaluation of algorithm performance in chip-seq peak detection. *PIOS One* (2012)
- Pepke, S., Wold, B., Ali, M.: Computation for chip-seq nad rna-seq studies. *Nature* (2009)
- Zhang, Y., Liu, T., Meyer, C.A., Eeckhoutte, J., Johnson, D., Bernstein, B., Nausbam, C., Myers, R.M., Brown, M., Li, W., Liu, X.S.: Model-based analysis of chip-seq (macs). *Genome Biology* (2008)
- Ji, H., Jiang, H., Ma, W., Johnson, D.S., Myers, R.M., Wong, W.H.: An integrated software system for analyzing chip-chip and chip-seq data. *Nature biotechnology* (2008)
- Kuan, P.F., Chung, D., Pan, G., Thomson, J.A., Stewart, R., Keleş, S.: A statistical framework for the analysis of chip-seq data. *Journal of the American Statistical Association* (2009)
- Lun, D.S., Sherid, A., Weined, B., Sherman, D.R., Galagan, J.E.: A blind deconvolution approach to high-resolution mapping of transcription factor binding sites from chip-seq data. *Genome Biology* (2009)
- Guo, Y., Mahony, S., Gifford, D.K.: High resolution genome wide binding event finding and motif discovery reveals transcription factor spatial bindings constraints. *PIOS, Computational Biology* (2012)
- Guo, Y., Papachristoudis, G., Altschuler, R.C., Gerber, G.K., Jaakkola, T.S., Gifford, D.K., Mahony, S.: Discovering homotypic binding events at high spatial resolution. *Bioinformatics* (2010)
- Zhang, X., Robertson, G., Krzowski, M., Ning, K., Droit, A., Jones, S., Gottardo, R.: Pics: Probabilistic inference for chip-seq. *Biometrics* (2010)
- Mendoza-Vargas, A., Olvera, L., Olvera, M., Grande, R., Vega-Alvarado, L., Taboada, B., Jimenez-Jacinto, V., Salgado, H., Juárez, K., Contreras-Moreira, B., Huerta, A.M., Collado-Vides, J., Morett, E.: Genome-wide identification of transcription start sites, promotes and transcription factor binding sites in e. coli. *PLOS one* (2009)
- Salgado, H., Peralta-Gil, M., Gama-Castro, S., Santos-Zavaleta, A., Muñiz-Rascado, L., García-Sotelo, J.S., Weiss, V., Solano-Lira, H., Martínez-Flores, I., Medina-Rivera, A., Salgado-Orsorio, G., Alquicira-Hernández, S., Alquicira-Hernández, K., López-Fuentes, P.-S.L. Alejandra, Huerta, A.M., Bonavides-Martínez, C., Balderas-Martínez, Y.I., Pannier, L., Olvera, M., Labastida, A., Jiménez-Jacinto, V., Vega-Alvarado, L., del Moral-Chávez, V., Hernández-Alvarez, A., Morett, E., Collado-Vides, J.: Regulondb v8.0: omics data sets, evolutionary conservation, regulatory phrases, cross-validated gold standards and more
- Planet, E., Attolini, C.S.-O., Reina, O., Rosell, D.: htseqtools: high-throughput sequencing quality control, processing and visualization in r. *Bioinformatics* (2011)
- Mendenhall, E.M., Bernstein, B.E.: Dna-protein interactions in high definition. *Genome Biology* (2012)
- Irizarry, R., Hobbs, B., Collin, F., Beazer-Barclay, Y., Antonellis, K., Scherf, U., Speed, T.: Exploration, normalization, and summaries of high density oligonucleotide array probe level data. *Biostatistics* (2003)
- Bolstad, B., Irizarry, R., Åstrand, M., Speed, T.: A comparison of normalization methods for high density oligonucleotide array data based on variance and bias. *Bioinformatics* (2003)
- ChIP-seq, beyond: new, improved methodologies to detect, characterize protein-DNA interactions: Furey, terrence s. *Nature Reviews: Genetics* (2012)

Supplement

Additional Enrichment plots for σ^{70}

In figure 8 it is shown the same relationship as in figure 3, but considering only regions formed where the reads are being allocated in more than 10 (A) and 30 (B) unique positions respectively. Both plots show that the vertical arms formed by regions with low ARC is formed by low complexity regions, that way suggesting that this segment correspond to the background of a ChIP-exo experiment.

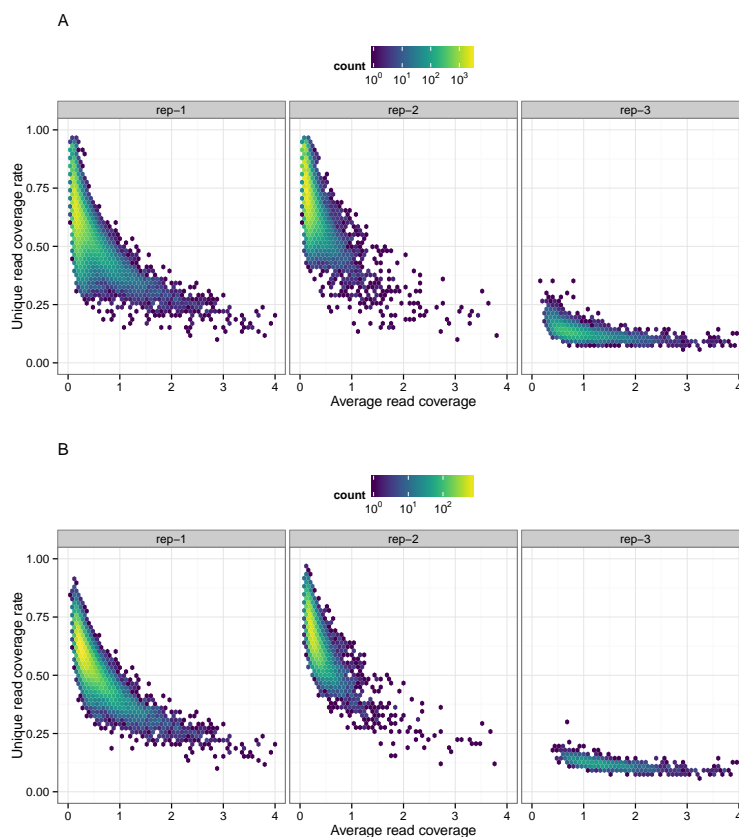


Figure 8 Hexbin plots of ARC vs URCR for each region after partitioning the genome. In A and B the regions with reads mapped to at most 10 and 30 positions respectively were not considered. ARC is defined as the ratio of the nr. of reads and the width of a region and URCR is the ratio of the number of unique position where the reads are being allocated and the number of reads in a region.